ICARUS 109, 133–144 (1994)

Near-Infrared Spectroscopy of Primitive Solar System Objects

JANE LUU[1,2]

Physics Department, Stanford University, Stanford, California 94305
E-mail: luu@blinky.stanford.edu

DAVID JEWITT[1]

Institute for Astronomy, University of Hawaii, Honolulu, Hawaii 96822

AND

EDWARD CLOUTIS

4 Huntstrom Rd, N. E., Calgary, Alberta, Canada T2K 5W3

Received November 1, 1993; revised March 1, 1994

We have obtained near-infrared (H and K band at $\lambda/\Delta\lambda \sim 480$ to 600) spectra of a sample of primitive objects including 2 Centaur objects (2060 Chiron and 5145 Pholus) and 16 P- and D-type asteroids. The spectra were obtained at the United Kingdom Infrared Telescope using the cooled grating spectrometer CGS4, and were used to search for chemically diagnostic vibrational features in these primitive objects. Pholus exhibits broad adsorption features at 2.07 and 2.27 μm, as well as a weak feature at 1.72 μm. The 1.72- and 2.27-μm features are similar to those seen in a laboratory tar sand sample. No distinct absorption features are found in other objects, including Chiron, which displays a spectrally neutral continuum. A comparison of the P- and D-type asteroid spectra with laboratory measurements of organic solids shows no compelling evidence for hydrocarbon overtones seen in terrestrial bituminous tar sands. © 1994 Academic Press, Inc.

1. INTRODUCTION

We are conducting a spectroscopic survey of primitive objects in the solar system, including cometary nuclei (Luu 1993) and potentially related objects such as Centaur objects, Trojan asteroids (Jewitt and Luu 1990), and near-Earth asteroids (NEAs) (Luu and Jewitt 1989). Our earlier work concentrated on the optical region of the spectrum because the signal-to-noise (S/N) ratios there are relatively high. The natural next phase of the survey is to extend the spectral coverage to the near-infrared region in which prominent vibrational features occur. In this paper, we concentrate on near-infrared spectral properties of distant primitive objects, including the Centaur objects 2060 Chiron and 5145 Pholus, and the P- and D-type asteroids.

Chiron and Pholus belong to the Centaur group, distant objects postulated to be relatively new to the planetary region. Their chaotic orbits in the Saturn–Uranus region imply that they must have arrived fairly recently at their current locations from a source in the outer solar system, possibly the Kuiper belt of comets (Tremaine 1990, Luu 1993). They are believed to have undergone less thermal evolution than other small solar system bodies due to their large heliocentric distances. Their hypothesized origin in the outer solar system suggests a composition containing simple hydrocarbons thought to be common in the outer solar system (Cruikshank 1987). This hypothesis is consistent with the albedos of Chiron (geometric albedo ≥ 4%, Jewitt and Luu 1992), and Pholus (maximum albedo 0.044 ± 0.013, Davies *et al.* 1993a). The presence of near-surface volatiles in Chiron is borne out by its cometary activity (e.g., Luu and Jewitt 1990, Bus *et al.* 1991); Pholus has shown no visible signs of sublimation but its distant location also suggests a volatile-rich composition.

The P- and D-type asteroids dominate the L4 and L5 Trojan clouds of Jupiter and the outer parts of the main belt. They are held to be among the most primitive of the known asteroid types (Bell *et al.* 1989). Their large heliocentric distances imply low condensation temperatures (<350 K, Bell *et al.* 1989). Three-micrometer observations of these asteroids provide no evidence for water of hydration, raising the possibility that water is incorporated in these bodies as buried ice (Jones *et al.* 1990; Lebofsky *et al.* 1990). The visual geometric albedos are of order a few percent (Gradie and Veverka 1980), while

---

[1] Guest Observer at the United Kingdom Infrared Telescope.

[2] Hubble Fellow.

0019-1035/94 $6.00

the visible colors are substantially redder than sunlight (Zellner *et al.* 1985; Jewitt and Luu 1990). These observations have again been taken to suggest that the surfaces contain organic materials (Gradie and Veverka 1980; Cruikshank 1987).

The fundamental bands and strongest overtones of likely organic surface materials occur in the near-infrared region of the reflection spectrum (e.g., Cloutis 1989). However, spectral observations in this region have traditionally been difficult. Their low albedos and large distances render most P- and D-objects too faint for high S/N spectral observations. Published broadband photometry is compatible with organic-rich surface compositions (e.g., Hartmann *et al.* 1982, Smith *et al.* 1992), but lacks the spectral resolution needed to reveal discrete features due to particular hydrocarbons. Spectral evidence is very limited. There is an unconfirmed report of the presence of the C–H vibrational band at 3.4 μm (Cruikshank and Brown 1987), and a C–N vibrational overtone at 2.2 μm has been recently reported in spectral observations at resolution $\lambda/\Delta\lambda \sim 45$ (Cruikshank *et al.* 1991).

We wish to test the validity of the claim regarding organic materials in outer solar system objects. To that purpose, this paper presents new near-infrared spectral observations of 2060 Chiron, 5145 Pholus, and P- and D-type asteroids. The spectra sample reflected sunlight in the H (1.4–1.8 μm) and K (2.05–2.45 μm) bands, and hold the potential for revealing previously unseen materials on these primitive bodies.

2. OBSERVATIONS

The present observations were taken in January and April 1993 at the 3.8-m diameter United Kingdom Infrared Telescope (UKIRT) on Mauna Kea, Hawaii. The cooled grating spectrograph CGS4 was mounted at the Cassegrain focus. The detector was a 58 × 62 pixel InSb array, with a read-out noise of 40 electrons. For all observations, we employed a 75 line per mm grating in the first order. The resulting dispersion was 34 Å/pixel at H ($\lambda/\Delta\lambda \sim 480$) and K ($\lambda/\Delta\lambda \sim 600$), while the pixel scale was 3.08 arcsec per pixel in the direction perpendicular to the dispersion. Nyquist sampling of the spectra was achieved by shifting the detector by $\frac{1}{2}$ pixel (17 Å) in the dispersion direction on alternate integrations. The 3 × 80 arcsec entrance slit was aligned north–south on the sky. The image quality was typically ~1 arcsec, small compared to the slit width, so that 95% of the light fell within a single pixel in the spatial direction. An optical TV camera, fed by a dichroic beam splitter, was used for target acquisition and guiding. Flat fields and wavelength calibration spectra were obtained on each night of observation.

All observations were restricted to small airmass to minimize differential atmospheric refraction. The identity of each target was confirmed by noting its motion relative to the fixed stars. The target was located and centered to better than 0.5 arcsec in the guider TV. The infrared and optical centers of the spectrometer and the TV camera were aligned prior to each measurement, using nearby G and K stars at equal airmass (airmass difference <0.05). The sky background was subtracted by nodding the telescope 24.6 arcsec (8 pixels) along the slit every 30 sec. Cumulative integration times were varied according to the brightness of the object, ranging from 20 min to ~2 hr. The CGS4 spectrometer records the H and K spectral regions at separate times, allowing the possibility that the targets may vary in brightness (due to rotation) between the H and K observations. Therefore, we are less certain of the absolute H–K color than of the spectral slopes within the H and K bands. Generally, the H and K spectra appear to connect smoothly, suggesting that rotational variations in most of the observed asteroids are modest. Reflectivity spectra were computed from nightly observations of the prime solar analog 16 Cyg B (Hardorp 1978, 1980).

Our sample contains 16 asteroids (including 5 P-types and 8 D-types), plus 2060 Chiron and 5145 Pholus. Details from the observing log are given in Table I.

3. DATA REDUCTION

In the 1–2.5 μm region, the principal absorbing gases in the atmosphere are water vapor and carbon dioxide (Zuev 1974). The effects of atmospheric extinction in the near infrared are evident in Fig. 1, which shows the ratios

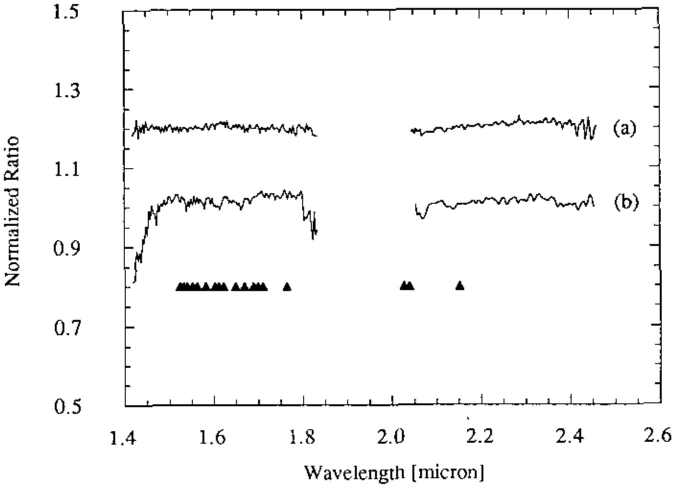

FIG. 1. Normalized ratio of two spectra of solar analog 16 Cyg B. (a) Ratio of two spectra taken on 24 Apr (airmass 1.18), and on 25 Apr (airmass 1.17). Both the H and K bands deviate from unity only at the ~1% level. (b) Ratio of two spectra taken on the same night, at airmasses 1.56 and 1.17. The ends of the H band deviate from unity at the 10–20% level, showing the importance of correcting for atmospheric correction. The triangles mark the wavelengths of especially strong airglow lines.

TABLE I
Observation Log

Name	Type	Group	V	Date	R (AU)	Δ (AU)	α (°)
2060 Chiron	—	Centaur	15.7	1993 Jan 21	9.35	8.43	−2.21
5145 Pholus	—	Centaur	16.8	1993 Jan 20	8.94	8.01	−2.03
46 Hestia	P	Main belt	12.6	1993 Apr 26	2.68	1.78	−12.1
190 Ismene	P	Main belt	14.5	1993 Apr 24	4.60	3.88	−9.6
336 Lacadiera	D	Main belt	13.8	1993 Apr 26	2.04	1.72	−29.5
406 Erna	P	Main belt	15.6	1993 Apr 25	3.40	2.50	8.9
613 Genevre	P	Main belt	15.0	1993 Apr 25	2.94	2.50	19.2
617 Patroclus	P	Trojan	15.9	1993 Jan 21	5.76	4.89	−4.9
659 Nestor	XC	Trojan	16.1	1993 Apr 24	5.25	4.30	−3.9
773 Irmintraud	D	Main belt	13.3	1993 Apr 24	2.81	1.87	8.5
884 Priamus	D	Trojan	16.1	1993 Jan 21	5.72	4.74	1.1
1143 Odysseus	D	Trojan	15.8	1993 Apr 25	5.71	5.03	−8.0
1172 Aneas	D	Trojan	15.8	1993 Jan 21	5.68	4.74	−3.1
1208 Troilus	FCU	Trojan	16.7	1993 Jan 21	5.64	4.90	−7.1
			17.1	1993 Apr 24	5.66	5.40	10.1
1583 Antilochus	D	Trojan	16.0	1993 Apr 26	5.35	4.50	−6.3
2241 Alcathous	D	Trojan	15.8	1993 Jan 20	5.24	4.32	4.2
2375 1975AA	D	Main belt	14.2	1993 Apr 26	2.48	1.54	11.2
2797 Teucer	—	Trojan	15.8	1993 Apr 25	5.39	4.54	−6.2

of spectra of 16 Cyg B taken at different airmasses (1.56 vs 1.17). Selective extinction is clear when spectra taken at different airmasses are compared, especially in the wings of the H band. Extinction is larger in the H band (cf. McCord and Clark 1979), and the spectrum at high airmass tends to be distorted shortward of ~1.45 μm and longward of 1.8 μm. There is little or no distortion in the K band (at the ~1% level), even with a relatively large airmass difference. Spectral distortion was minimized by dividing each asteroid spectrum by a spectrum of 16 Cyg B taken at similar airmass (Δairmass < 0.2).

The infrared airglow is an independent source of error, and is especially large in the H band. Wavelengths of strong airglow lines (Ramsey *et al.* 1992) are marked for reference in Fig. 1. Subtraction of the night sky emission was generally successful, as can be seen in most asteroid spectra (e. g., Fig. 2). Small residuals apparent in the sky-subtracted spectra are presumably due to changes in the sky brightness on timescales short compared to the 30-sec nodding frequency of the telescope (Ramsay *et al.* 1992). Small errors may also result from imperfect alignment of the night sky lines with the columns in the CGS4 detector. In the brightest objects, the residual sky lines (as opposed to random noise) limit the accuracy with which we can locate the asteroid continuum.

The reflectivity spectra of the asteroids are shown in Fig. 2, while those of Chiron and Pholus are shown in Fig. 3. All reflectivities were normalized to unity at 2.2 μm and smoothed to 68 Å (2 pixel) resolution. The plotted reflectivities have S/N in the range 20–100 per resolution element and, with the exception of 5145 Pholus, show smooth, featureless continua. Pholus shows absorption bands at 1.72, 2.07, and 2.27 μm. Where there are no apparent spectral features, limits on the presence of possible features were determined by fitting and subtracting the continuum from each spectrum. The fitting function was a cubic spline in first order applied to the entire data range. The residuals are shown in Fig. 4. As shown in the figure, the residuals fluctuate about a mean of zero for all observed asteroids and Chiron, indicating that, within the noise, there were no apparent spectral features.

4. DISCUSSION

Comparison with Laboratory Samples

We attempted to investigate the compositions of the observed objects by comparing the telescopic spectra with laboratory spectra of various dark materials, including tar sands, carbon lampblack, coal, coal tar extract, oil shale, graphite, and one carbonaceous chondrite (CR chondrite). These materials were chosen because they should serve as reasonable spectral analogs for primitive objects like Trojan asteroids and cometary nuclei (Gradie and Veverka 1980), and because good laboratory reflectance spectra are available for them (Cloutis 1989). The organic phase of these materials is composed largely of polycyclic aromatic hydrocarbons (PAHs), as is the bulk of the organic phase in carbonaceous chondrites. Their organic phase is also contained in media which are spectrally

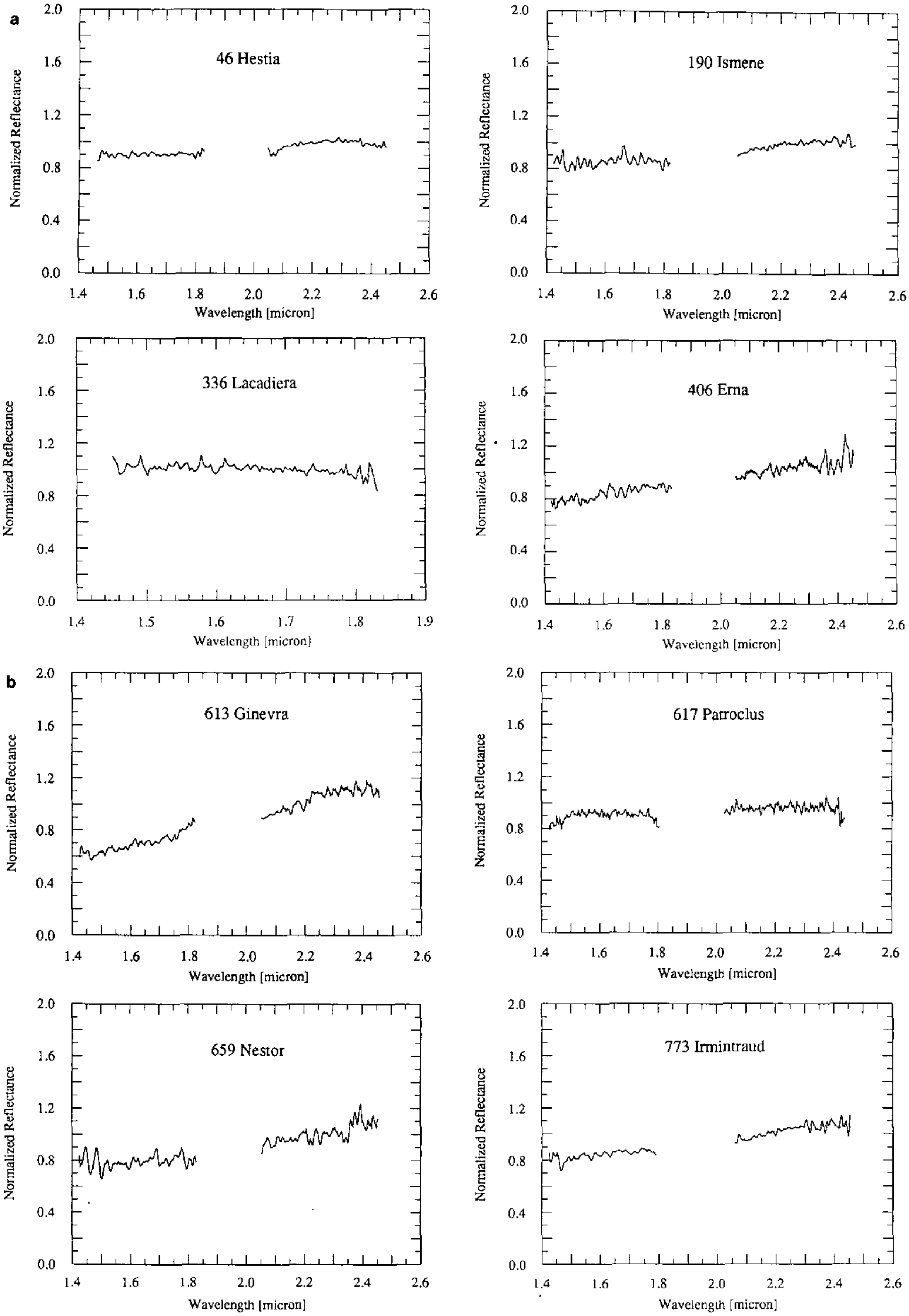

FIG. 2. Reflectance spectra of observed asteroids, normalized at 2.2 μm and plotted on a common scale.

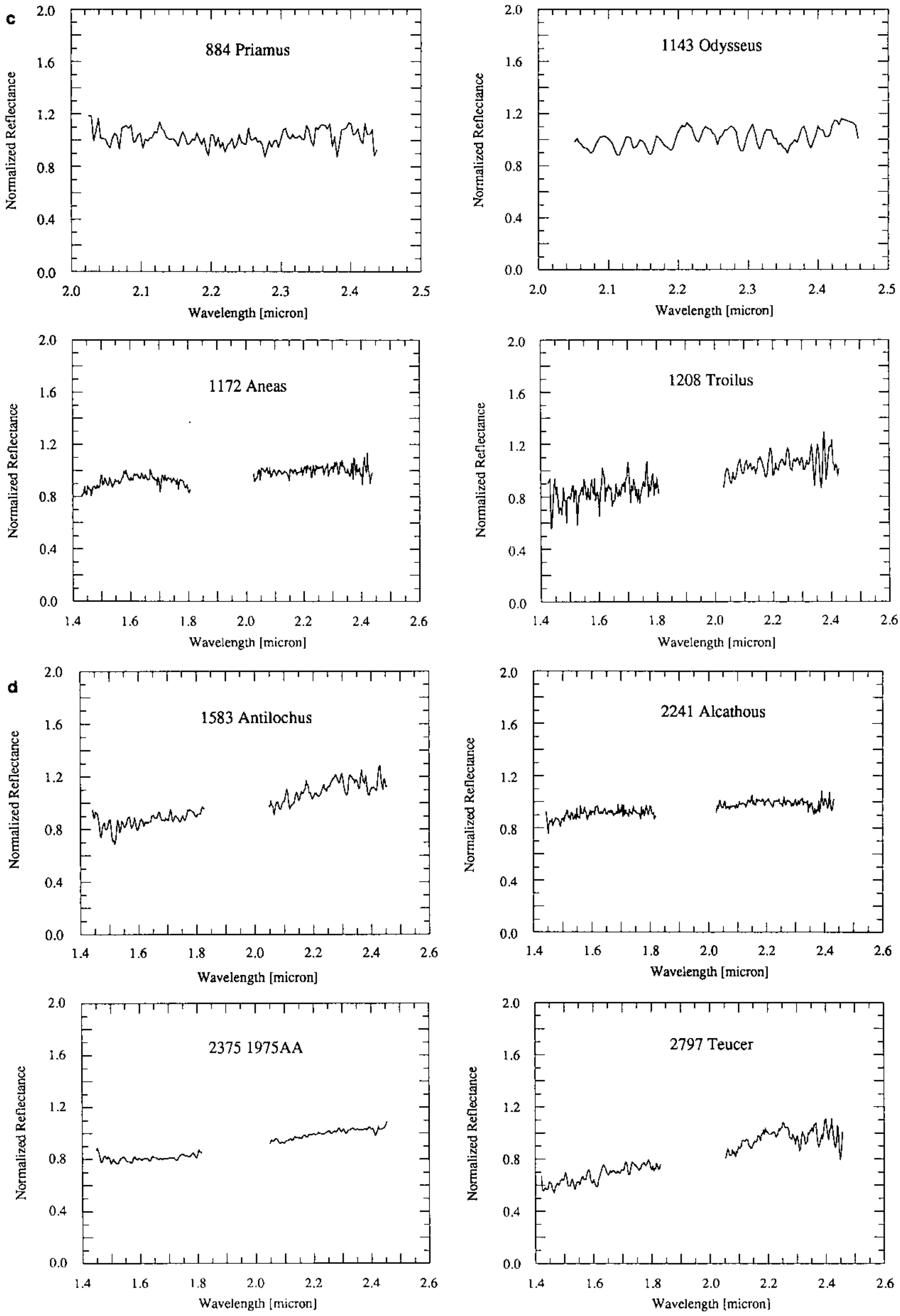

FIG. 2.—*Continued*

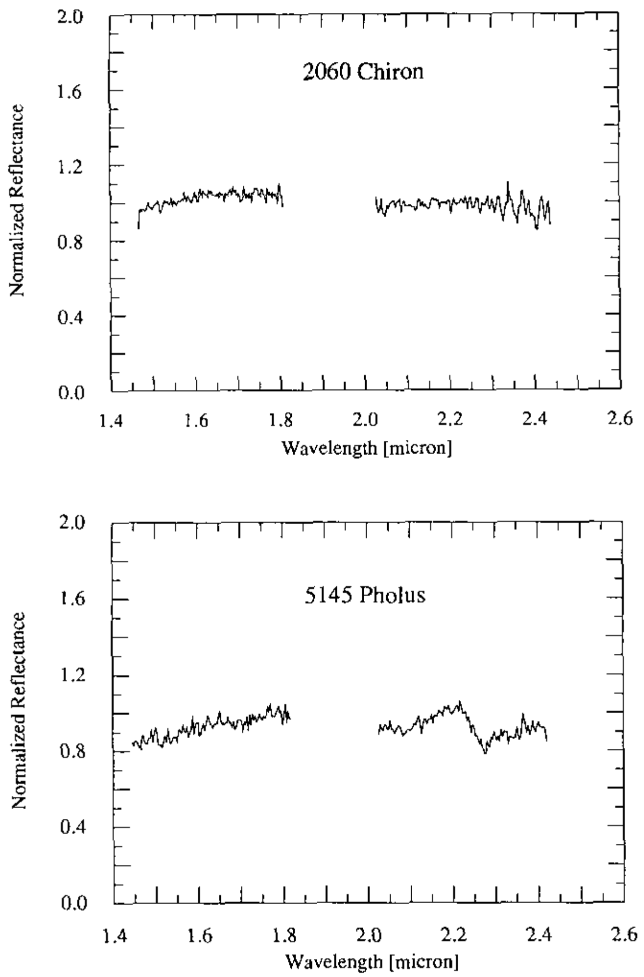

FIG. 3. Reflectivity spectra of (top) 2060 Chiron and (bottom) 5145 Pholus, both normalized at 2.2 μm and plotted on a common scale. The Chiron spectrum is featureless, while that of Pholus shows broad absorption features at 2.07 and 2.27 μm, and a weak one at 1.72 μm.

neutral (e.g., quartz sand in tar sand samples), eliminating the possibility of confusing spectral signatures. The CR chondrite is believed to be more primitive than other carbonaceous chondrites (Mason and Wiik 1962). In general, organic material from other meteorites was not used in the comparison because of the large volume of sample needed (~1 g), and because there is some evidence that the composition and structure of the organic phase is altered in the extraction process of a large mass of carbonaceous chondrite. Furthermore, the available spectra of carbonaceous chrondrite organic material (Bell *et al.* 1985, Cruikshank 1987) exhibit fairly flat reflectivity gradients which are more characteristic of C-type asteroids than P- and D-type asteroids. Finally, we acknowledge that there may be better complex organics which might have histories more similar to primitive solar system objects. However, the history of these objects is poorly constrained, and so many scenarios of surface alteration are possible (e.g., T Tauri winds, solar winds) that it would be premature to focus on other surface materials beyond complex organics.

Tar sands are mixtures of clays, bitumen (a family of complex polymerized hydrocarbons), quartz grains, water, and minor accessory minerals (e.g., zircon, ilmenite) (Bichard 1987). The organic fractions in the tar sand and oil shale differ in fundamental respects. The tar sand organic fraction is composed predominantly of heterocyclic, solvent-soluble organic molecules, while the oil shale organic fraction is composed predominantly of cyclic, solvent-insoluble organic molecules (Boyd and Montgomery 1962, Tissot and Welte 1978). Carbon lampblack is a soot produced by burning carbon electrodes and contains amorphous carbon. Coal tar extracts differs from coal in that it has had the soluble organic fraction removed and consists of insoluble aromatics. Overall, 29 laboratory spectra were available for comparison, of which 7 were found to provide reasonably good matches to the telescopic spectra. These 7 laboratory spectra are shown in Fig. 5 and a brief note on the origin of each sample can be found in Table II.

We used the chi-squared test (e.g., Mendenhall *et al.* 1986) to measure the goodness of fit between the 7 laboratory spectra and the telescopic spectra, since random errors in the measurements were assumed to dominate over systematic errors. The test was not used to identify the composition of an object in an absolute sense. Rather, we used the chi-squared values only for *relative* comparison, i.e., to determine whether one particular laboratory

TABLE II
Sample Identification and Description

	Grain size		Absolute reflectance	
Sample name	% < 45 μm	% > 45 μm	0.56 μm	2.0 μm
Tar sand 6	3.8	92.8	—	—
CR meteorite	100	0	—	—
Synthetic "amorphous" graphite	100	0	1–8%	—
Oil shale	100	0	14%	25%
Coal	—	—	2.5%	25%
Coal tar extract	100	0	1–8%	—
Carbon lamb black	100	0	1–8%	—

Note. All tar sands are from the Fort McMurray, Alberta, area. The tar sand 6 spectrum is of an unsorted sample. The CR meteorite is sample EET87770,19 (Antarctica) and was crushed to size <45 μm. The synthetic "amorphous" graphite is more amorphous than natural graphite. The oil shale is from near Rifle, Colorado, and was crushed to <45 μm grain size. The coal sample is a bituminous coal from near Frank, Alberta, and was crushed to <37 μm grain size. The coal tar extract is from Jeff Bell (Univ. of Hawaii), and is the same material as used in Bell *et al.* (1985).

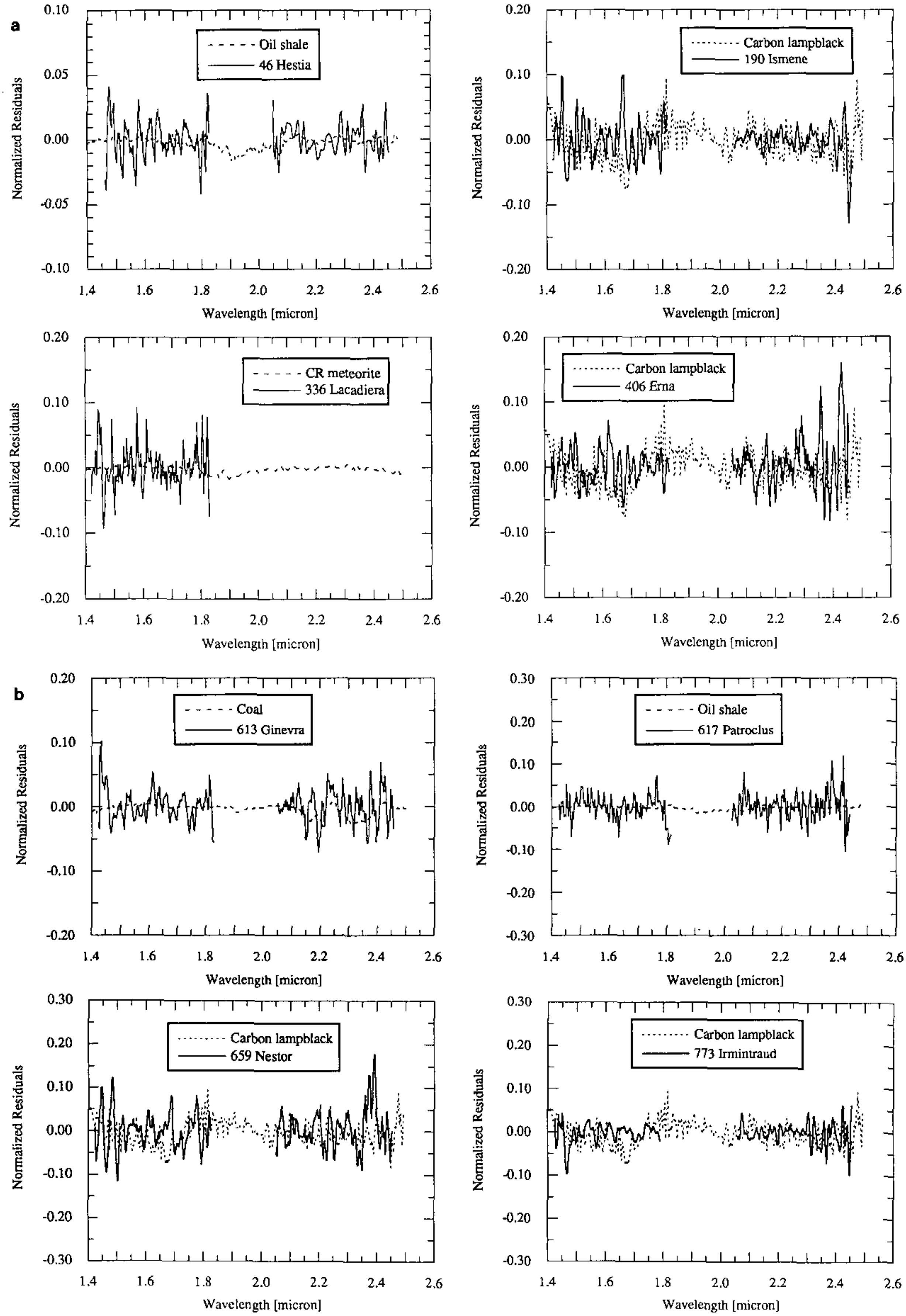

FIG. 4. Residuals in the object spectra and the best-fitting laboratory spectra after the continua have been fitted and subtracted.

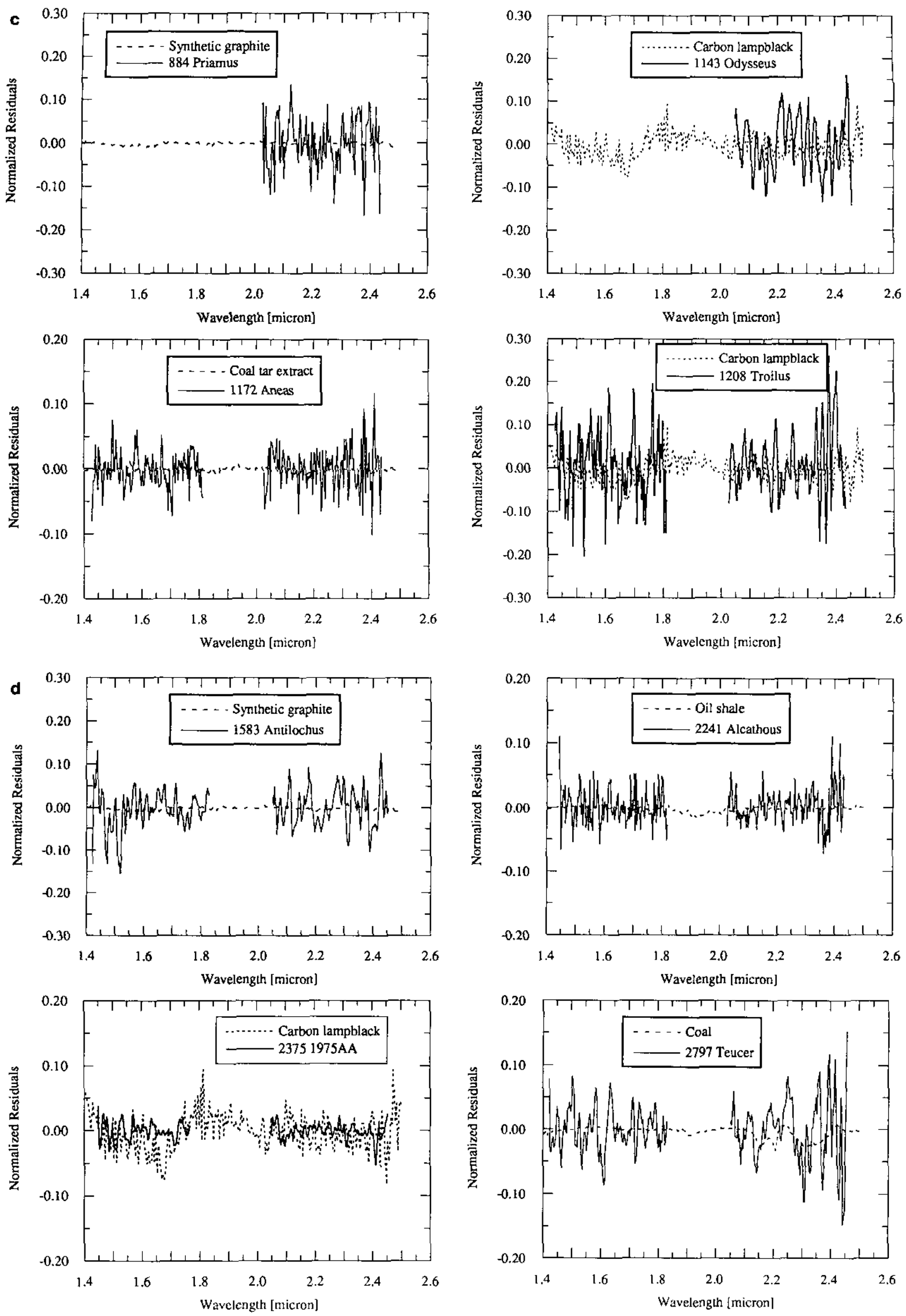

FIG. 4.—*Continued*

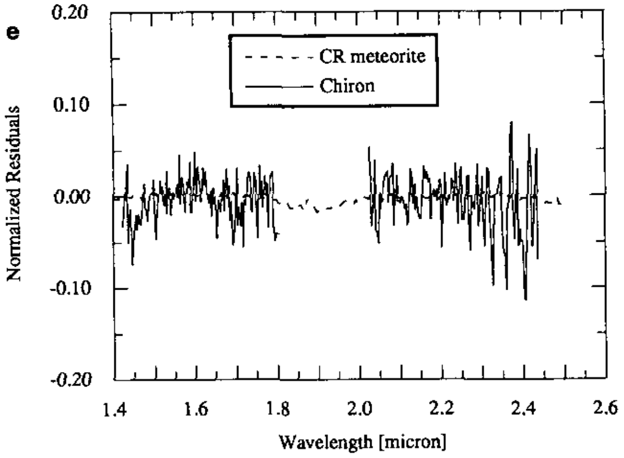

FIG. 4—*Continued*

TABLE III
Best Matching Spectra

Name	Type	Group	Best matching laboratory sample
2060 Chiron	—	Centaur	CR meteorite
5145 Pholus	—	Centaur	Tar sand 6
46 Hestia	P	Main belt	Oil shale
190 Ismene	P	Main belt	Carbon lampblack
336 Lacadiera	D	Main belt	CR meteorite (H band only)
406 Erna	P	Main belt	Carbon lampblack
613 Ginevra	P	Main belt	Coal
617 Patroclus	P	Trojan	Oil shale
659 Nestor	XC	Trojan	Carbon lampblack
773 Irmintraud	D	Main belt	Carbon lampblack
884 Priamus	D	Trojan	Synthetic graphite (K band only)
1143 Odysseus	D	Trojan	Carbon lampblack
1172 Aneas	D	Trojan	Coal tar extract
1208 Troilus	FCU	Trojan	Carbon lampblack
1583 Antilochus	D	Trojan	Synthetic graphite
2241 Alcathous	D	Trojan	Oil shale
2375 1975AA	D	Main belt	Carbon lampblack
2797 Teucer	—	Trojan	Coal

sample provided a better fit than another. The results from the tests are shown in Table III, and the goodness of fit for each match can be seen in the residual plots of Fig. 4.

We are aware that laboratory reflectance spectra can produce slightly different results from telescopic observations due to different photometric geometries (Gradie and Veverka 1982), and that rigorous comparison between the two types of reflectance spectra generally invoke some theoretical model of scattering (e.g., Hapke 1981). However, we believe that, in the case of the spectra presented here, the effects due to different observation techniques are small for the following reasons: (1) both the telescopic spectra and the lab spectra were taken at small phase angles ($\leq$12° for all but two objects, 15° for the lab spectra); (2) our targets are dark. Geometric effects are small ($\leq$3%) and likely to be unimportant for dark objects (Gradie and Veverka 1982).

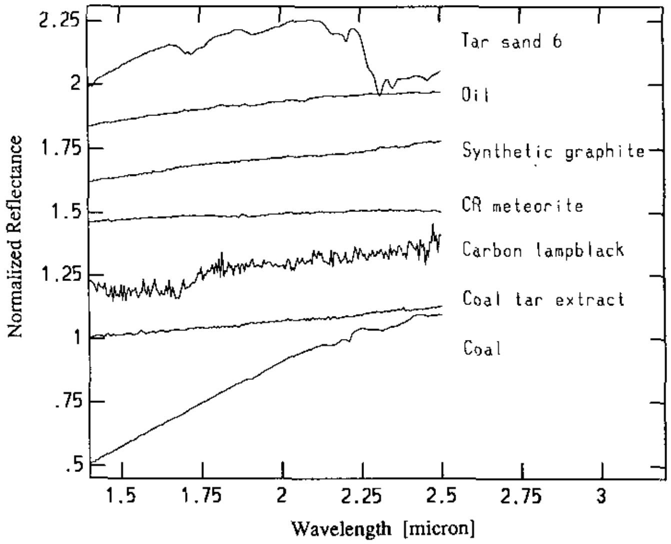

FIG. 5. Reflectance spectra of the seven laboratory samples which provided the best fits to the object spectra.

Numerous overtones and combination bands of hydrocarbon bonds fall in the observed spectral windows. In the laboratory samples discussed by Cloutis (1989), the more prominent absorptions have band depths $\sim$10 to 50% of the local continuum, and would be clearly visible in the present data. Their absence in the P- and D- asteroid spectra probably indicates a genuine lack of organic materials containing significant amounts of aliphatic CH, CH_2, and CH_3 groups in these objects (this conclusion only applies to the depth to which near-IR spectroscopy might be expected to sample the surface of these bodies, i. e., $<$1 mm). Alternatively, organics may be present, but their spectral features may be diluted by contamination with low-albedo, spectrally bland matter. A similar case exists in spectra of the dark hemisphere of Iapetus, which is thought to be coated in hydrocarbons and yet which fails to show characteristic spectral features of aliphatic organics in the near-infrared (Bell *et al.* 1985; Cloutis 1989). Low-bitumen terrestrial tar-sands provide an approximate match to the featureless Iapetus spectrum (Cloutis 1989). Similar materials on the P- and D- asteroid spectra and having a very low bitumen content ($<$3%) would likewise escape detection in the present data.

Main Belt and Trojan Asteroids

Although there is no unambiguous evidence for spectral features, the spectra of some asteroids (e.g., 659 Nestor,

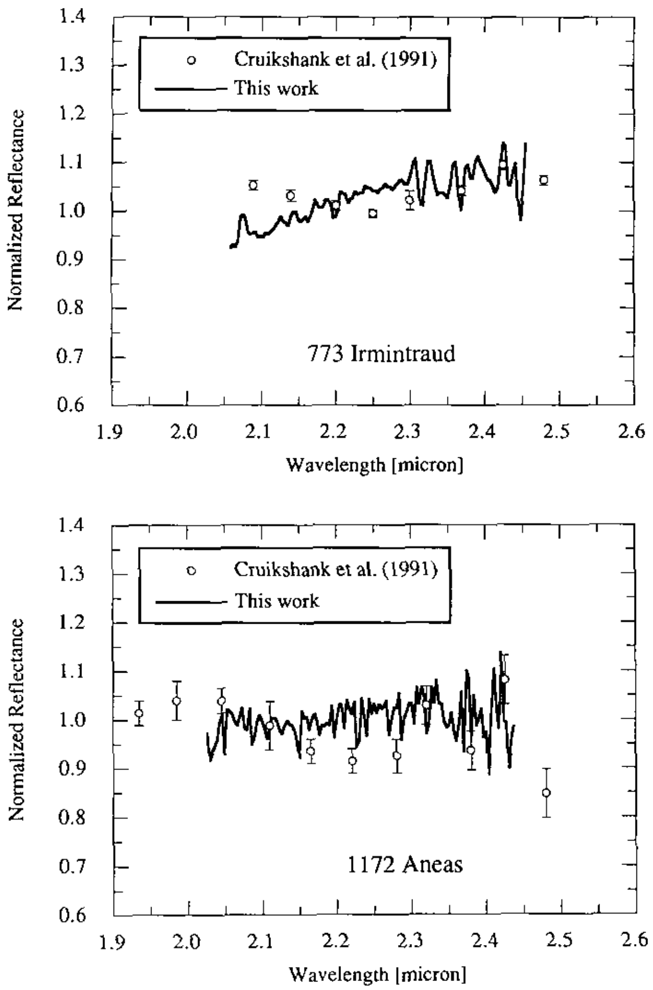

FIG. 6. CGS4 spectra of D-type asteroids (a) 773 Irmintraud and (b) 1172 Aneas compared with earlier data. There is no sign of the 2.24 μm feature reported by Cruikshank *et al.* (1991).

2797 Teucer) suggest weak features in the 2.30–2.35 μm region (see Fig. 2). This region corresponds to the strongest combination bands involving CH_2 and CH_3 functional groups (Cloutis 1989, 1990). From the spectra, we place an upper limit of $<10\%$ on the depths of these tentative bands, implying an upper limit of <3 wt% bitumen (assuming the organic fraction to be similar to that in tar sand). The bitumen content of these asteroids could exceed ~3 wt% if their organic fractions are more depleted in CH_2 and CH_3 groups than tar sand, as is the case for the macromolecular, solvent-insoluble fraction found in carbonaceous chondrites (Hayatsu and Anders 1981).

Asteroids 773 Irmintraud and 1172 Aneas (both D-types) were cited by Cruikshank *et al.* (1991) as showing an overtone of the C–N vibration at 2.2 μm. In Fig. 6, we compare our CGS4 spectra of these asteroids with the earlier data from Cruikshank *et al.* The CGS4 spectra of 773 Irmintraud and 1172 Aneas provide no evidence for the reported feature. Specifically, no absorption deeper than ~3% is present in the spectra of these objects. Spectra obtained by Howell *et al.* (1992) also failed to show a 2.2-μm feature in 773 Irmintraud. The C–N fundamental absorption band at 4.7 μm should be deeper than the 2.2-μm overtone, and would at first sight represent a more suitable observational target. However, ground-based observations at this wavelength are extremely difficult due to the high thermal background.

2060 Chiron and 5145 Pholus

The spectrum of Pholus was the only one to show unambiguous spectral features. We confirm the presence of broad absorption features at 2.07 and 2.27 μm first reported by Davies *et al.* (1993b); in addition, the high S/N of our spectrum also shows a weak feature at ~1.72 μm. Figure 7 shows a comparison of the Pholus spectrum with spectra of several common ices (CO_2, CH_4, H_2O, NH_3) in a first order attempt at identifying its features. NH_3 shows deep absorption features at ~2.02 and ~2.27 μm, similar to those in Pholus, but also possesses other

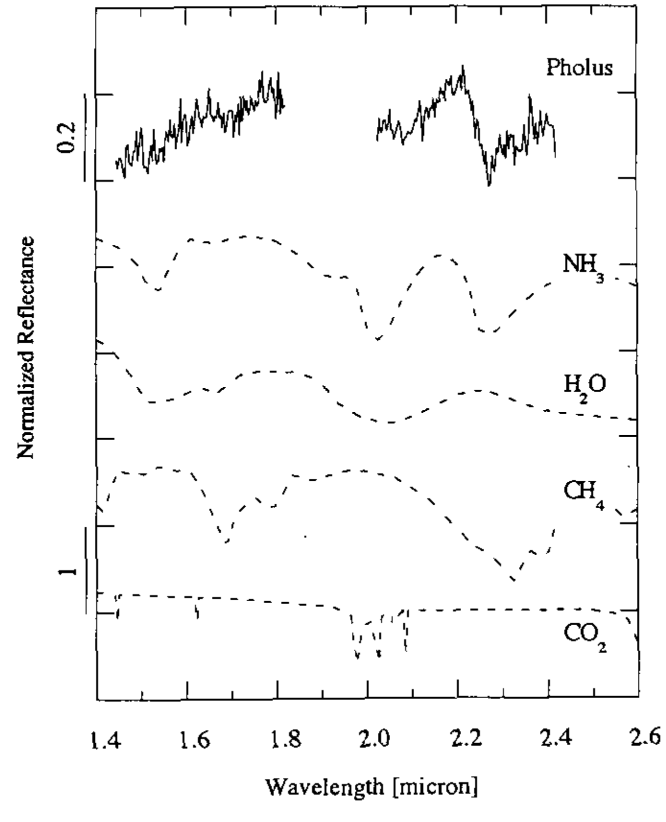

FIG. 7. Reflectance spectrum of 5145 Pholus compared with laboratory reflection spectra of ammonia (NH_3), water (H_2O), methane (CH_4), and carbon dioxide (CO_2) ices. The spectra have been normalized to unity at 2.2 μm, and are vertically offset for clarity of presentation. The spectrum of Pholus is shown at five times the vertical scale of the ice spectra, as indicated on the left axis.

features which are not reproduced in Pholus. In particular, the NH_3 reflectivity minimum at 1.52 μm is absent in the Pholus spectrum. Therefore, we do not conclude that the surface of Pholus is coated with ammonia ice. However, it is possible that vibrations of N–H in an unspecified, more complex molecule are responsible for the features in the Pholus spectrum. The identity of the 2.07 μm feature in Pholus is unknown but might be attributable to an N–H functional group (Goddu and Delker 1960). There is no resemblance between Pholus and the spectra of other common ices.

A better fit to the Pholus spectrum was found in the laboratory sample Tar sand 6, as can be seen in Fig. 8. The Tar sand 6 sample is characterized by a large particle size (predominantly >45 μm) and a medium bitumen content (3.4%) (see Table II). Like Pholus, the sample exhibits absorptions near 1.7 and 2.3 μm, although the 2.07-μm feature is not present in the sample. In tar sand, the 2.27-μm band is tentatively identified as a combination of the overtones of the fundamental organic bands due to hydrocarbons: the asymmetric CH_3 stretch and the asymmetric CH_2, CH_3 bend (Cloutis 1989). Thus the features in Pholus may be the signatures of the following chemical groups: (1) an N–H functional group (based on the 2.07- and 2.27-μm features), and (2) a form of hydrocarbon (based on the 1.72- and 2.27-μm features), possibly in the form of bitumen (~a few percent). The latter would be consistent with the fact that the Pholus spectrum could also be matched by "Titan tholin," a nonvolatile organic residue obtained after evaporation of irradiated hydrocarbon-containing ice mixtures (Hoffman *et al.* 1993, Wilson *et al.* 1993). If the features can be attributed to hydrocarbons, they thus provide evidence for organic material on Pholus.

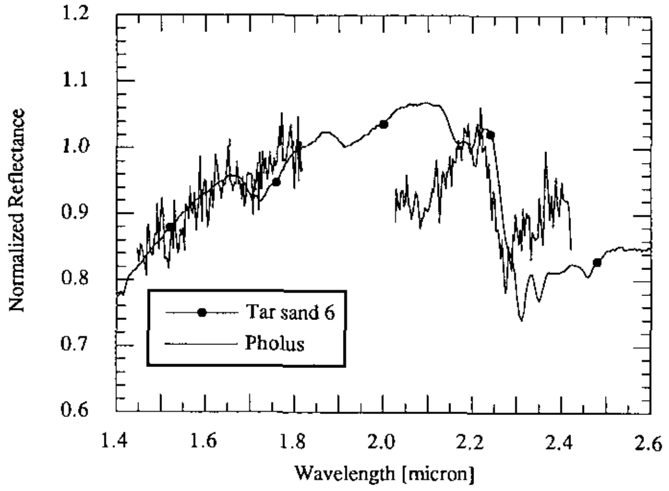

FIG. 8. Spectrum of Pholus compared with that of the best-fitting laboratory sample Tar sand 6.

The spectral features apparent in Pholus have no analogs in Chiron, consistent with the widely disparate optical colors of the two objects (Mueller *et al.* 1992, Fink *et al.* 1992, Binzel 1992, Luu 1993.) The cause of this dissimilarity is not known, but we hypothesize that it may be related to the fact that Chiron has shown cometary activity while Pholus has not. Assuming a common origin for both objects, cometary activity in Chiron may have altered its original mantle, while that of Pholus remains intact. Perhaps Chiron is covered by a layer of fall-back debris produced by outgassing, so that the irradiated mantle is buried. As was done for the asteroid spectra, limits to the possible presence of spectral features in Chiron were determined by fitting and subtracting the continuum. The results can be seen in Fig. 4.

5. SUMMARY

Reflection spectra of the distant objects 5145 Pholus and 2060 Chiron plus 16 outer main belt and Trojan asteroids were obtained in the H and K infrared spectral windows, at signal-to-noise ratios of 20–100 per 0.07-μm resolution element. We find that:

(1) The P- and D-type asteroid spectra are featureless at $S/N \geq 20$ in both H and K bands.

(2) The asteroids show no compelling evidence for hydrocarbon overtone and combination bands measured previously in terrestrial bituminous tar-sands (Cloutis 1989). Upper limits to the depths of possible bands suggest maximum organic carbon contents of <3 wt%. From the present study, we cannot eliminate the possibility that the P- and D-type asteroid surfaces are devoid of organics.

(3) We confirm the presence of absorption features at 2.07 and 2.27 μm in the spectrum of Pholus (cf. Davies *et al.* 1993b). The features are broad (~0.2 μm wide) and deep (~20%). In addition, we discovered another weak absorption feature at 1.72 μm. A partial match for the Pholus spectrum was found in a laboratory spectrum of tar sand (based on the 1.72- and 2.27-μm features), and also in NH_3 ice (based on the 2.07- and 2.27-μm features). If Pholus's 1.72- and 2.27-μm features can be attributed to hydrocarbons (as in tar sand), they indicate the presence of organic material on Pholus.

(4) The spectral features seen in Pholus have no analogs in Chiron. The Chiron spectrum is featureless in the observed region.

(5) We find no evidence for the 2.2-μm absorption feature reported in asteroids 773 Irmintraud and 1172 Aneas by Cruikshank *et al.* (1991), attributed by them to C–N.

ACKNOWLEDGMENTS

We thank Tom Geballe for an excellent introduction to the CGS4 and Thor Wold and Dolores Walther for their expert help at the telescope. We also thank Carle Pieters and Steve Pratt of Brown University for providing us with some of the laboratory spectra, and T. Jones and W. Grundy for helpful comments on the manuscript. JXL is supported by NASA through Grant HF-1035.01. −92A, awarded by the Space Telescope Science Institute, which is operated by the Association of Universities for Research in Astronomy, Inc., for NASA under Contract NAS5-26555. DCJ acknowledges support from the NASA Planetary Astronomy Program. EAC acknowledges support from the Alberta Oil Sands Technology and Research Authority.

REFERENCES

Bell, J. F., D. P. Cruikshank, and M. J. Gaffey 1985. The composition and origin of the Iapetus dark material. *Icarus* **61,** 192–207.

Bell, J. F., D. R. Davis, W. K. Hartmann, and M. J. Gaffey 1989. Asteroids: The big picture. In *Asteroids II* (R. P. Binzel, T. Gehrels, and M. Matthews, Eds.), pp. 921–945. Univ. of Arizona Press, Tucson.

Bichard, J. A. 1987. *Oil Sands Composition and Behaviour Research.* AOSTRA Tech. Publ. Ser., No. #4, AOSTRA, Edmonton.

Binzel, R. P. 1992. The optical spectrum of 5145 Pholus. *Icarus* **99,** 238–240.

Boyd, M. L., and D. S. Montgomery 1962. *A Study of the Athabasca Bitumen from the Abasand Quarry, Alberta, Canada.* Report 104, Department of Mines and Technical Surveys, Ottawa, Canada.

Bus, S. J., M. F. A'Hearn, D. G. Schleicher, and E. Bowell 1991. Detection of CN emission from (2060) Chiron. *Science* **251,** 774–777.

Cloutis, E. A. 1989. Spectral reflectance properties of hydrocarbons: Remote sensing applications. *Science* **245,** 165–168.

Cloutis, E. A. 1990. Identification, detection and characterization of individual tar sand phases using diffuse reflectance spectroscopy (0.35–2.6 μm). *AOSTRA J. Res.* **6,** 17–27.

Cruikshank, D. P. 1987. Dark matter in the solar system. *Adv. Space Res.* **7**(5), 109–120.

Cruikshank, D. P. and R. H. Brown 1987. Organic matter on asteroid 130 Elektra. *Science* **238,** 183–184.

Cruikshank D. P., L. J. Allamandola, W. K. Hartmann, D. J. Tholen, R. H. Brown, C. N. Matthews, and J. F. Bell 1991. Solid C–N bearing material on outer solar system bodies. *Icarus* **94,** 345–353.

Davies, J., J. Spencer, M. Sykes, D. Tholen, and S. Green 1993a. IAU Circular 5698.

Davies, J. K., M. V. Sykes, and D. P. Cruikshank 1993b. Near-infrared photometry and spectroscopy of the unusual minor planet 5145 Pholus (1992 AD). *Icarus* **102,** 166–169.

Fink, U., M. Hoffman, W. Grundy, M. Hicks, and W. Sears 1992. The steep red spectrum of 1992 AD: An asteroid covered with organic material? *Icarus* **97,** 145–149.

Goddu, R. F., and D. A. Delker 1960. Spectra–structure correlations for the near-infrared region. *Anal. Chem.* **32,** 140–141.

Gradie, J., and J. Veverka 1980. The composition of the Trojan asteroids. *Nature* **283,** 840–842.

Gradie, J., and J. Veverka 1982. When are spectral reflectance curves comparable? *Icarus* **49,** 109–119.

Hapke, B. 1981. Bidirectional reflectance spectroscopy. *J. Geophys. Res.* **86,** 3039–3054.

Hardorp, J. 1978. The Sun among the stars. I. A search for solar spectral analogs. *Astron. Astrophys.* **63,** 383–390.

Hardorp, J. 1980. The Sun among the stars. III. Energy distribution of 16 Northern G-type stars and the solar flux calibration. *Astron. Astrophys.* **91,** 221–232.

Hartmann, W. K., D. P. Cruikshank, and J. Degewij 1982. Remote comets and related bodies: VJHK colorimetry and surface materials. *Icarus* **52,** 377–408.

Hayatsu, R., and E. Anders 1981. Organic compounds in meteorites and their origins. *Top. Curr. Chem.* **99,** 1–37.

Hoffman, M., U. Fink, W. M. Grundy, and M. Hicks 1993. Photometric and spectroscopic observations of 5145 Pholus. *J. Geophys. Res. E* **98**(4), 7403–7407.

Howell, E. S., L. A. Lebofsky, M. C. Nolan, and E. M. Alvarez del Castillo 1992. Compositional trends among outer belt asteroids. *Bull. Am. Astron. Soc.* **24,** 941.

Jewitt, D. C., and J. X. Luu 1990. CCD spectra of asteroids. II. The Trojans as spectral analogs of cometary nuclei. *Astron. J.* **100,** 933–944.

Jewitt, D. C., and J. X. Luu 1992. Submillimeter continuum observations of 2060 Chiron. *Astron. J.* **104,** 398–404.

Jones, T. D., L. A. Lebofsky, J. S. Lewis, and M. S. Marley 1990. The composition and origin of the C, P, and D asteroids: Water as a tracer of thermal evolution in the outer belt. *Icarus* **88,** 172–192.

Lebofsky, L. A., T. D. Jones, P. D. Owensby, M. A. Feierberg, and G. J. Consolmagno 1990. The nature of low-albedo asteroids from 3-μm multi-color photometry. *Icarus* **83,** 16–26.

Luu, J. X. 1993. Spectral diversity in the nuclei of comets. *Icarus* **104,** 138–148.

Luu, J. X., and D. C. Jewitt 1989. CCD spectra of asteroids. I. Near–Earth and 3 : 1 resonance asteroids. *Astron. J.* **99,** 1985.

Luu, J. X., and D. C. Jewitt 1990. Cometary activity in 2060 Chiron. *Astron. J.* **100,** 913–932.

Mason, B., and H. B. Wiik 1962. *Am. Mus. Novit.* **2106,** 1–11.

McCord, T., and R. N. Clark 1979. Atmospheric extinction 0.65–2.50 μm above Mauna Kea. *Pub. Astron. Soc. Pacific* **91,** 571–576.

Mendenhall, W., R. L. Schaeffer and D. D. Wackerly 1986. *Mathematical Statistics with Applications,* pp. 612–618. Duxbury Press, Boston.

Mueller, B. E. A., D. J. Tholen, W. K. Hartmann, and D. P. Cruikshank 1992. Extraordinary colors of asteroidal object 1992 AD. *Icarus* **97,** 150–154.

Ramsay, S. K., C. M. Mountain, and T. R. Geballe 1992. Non-thermal emission in the atmosphere above Mauna Kea. *Mon. Not. R. Astron. Soc.* **259,** 751–760.

Smith, D. W., P. E. Johnson, W. L. Buckingham, and R. W. Shorthill 1992. JHK photometry of selected Trojan and Hilda asteroids. *Icarus* **99,** 485–488.

Tissot, B. P., and D. H. Welte 1978. *Petroleum Formation and Occurrence.* Springer-Verlag, Berlin.

Tremaine, S. 1990. Dark matter in the solar system. In *Baryonic Dark Matter* (D. Lynden-Bell and G. Gilmore, Eds.), pp. 37–65. Kluwer, Dordrecht.

Wilson, P. D., C. Sagan, and W. R. Thompson 1993. The organic surface of 5145 Pholus: Constraints set by scattering theory. Preprint.

Zellner, B., D. J. Tholen, and E. F. Tedesco, 1985. The eight-color asteroid survey: Results for 589 minor planets. *Icarus* **61,** 355–416.

Zuev, V. E. 1974. *Propagation of Visible and Infrared Radiation in the Atmosphere* (Transl. from Russian D. Lederman; P. Greenberg, Ed.). Wiley, New York.